Inorganic Chemistry
Article

Inorg. Chem. **2011**, *50*, 911–917 **911**
DOI: 10.1021/ic101490a

Temperature-Dependent in Situ Ligand Cyclization via C=C Coupling and Formation of a Spin-Crossover Iron(II) Coordination Polymer

Feng-Lei Yang, Jun Tao,* Rong-Bin Huang, and Lan-Sun Zheng

State Key Laboratory of Physical Chemistry of Solid Surfaces and Department of Chemistry, College of Chemistry and Chemical Engineering, Xiamen University, Xiamen 361005, People's Republic of China

Received July 26, 2010

The reaction of N^1,N^2-bis(pyridin-4-ylmethylene)ethane-1,2-diamine (**L**) with $Fe(NCS)_2$ under various temperatures gave rise to three iron(II) coordination polymers, namely, one-dimensional $[Fe(\mathbf{L}')(NCS)_2]$ (**1**), two-dimensional $[Fe(\mathbf{L})_2(NCS)_2]\cdot H_2O$ (**2**), and one-dimensional $[Fe(\mathbf{L})_2(NCS)_2]\cdot 2CH_2Cl_2\cdot 4MeOH$ (**3**). The formation of **1** involved an in situ C=C coupling reaction, **L** to **L′** [**L′** = 5,6-di(pyridin-4-yl)-1,2,3,4-tetrahydropyrazine], which was catalyzed by cyanide ions decomposed from thiocyanates; the manganese(II) (**1a**) and zinc(II) (**1b**) analogues of **1** were also synthesized for comparison. Magnetic studies showed that complex **1** underwent a pressure-dependent one-step incomplete spin transition whereas complexes **2** and **3** were paramagnetic in the whole temperature range.

Introduction

It is well-documented that in situ ligand reactions have led to the formation of plentiful coordination complexes with intriguing topological structures and physical properties[1] since the first one was proposed by Schröder et al. in 1997.[2] Up to now, in situ ligand reactions including C−C bond formation,[3] hydroxylation,[1a] alkylation,[1c] acylation,[1c] amination,[1c] decarboxylation,[1a] substitution,[1a] hydrolysis,[1a] transformation of inorganic sulfur into organic sulfur,[4] and tetrazole/triazole formation[1b] have been found, and many of them were carried out by photoirradiated or hydro(solvo)thermal methods. It is obvious that C−C bond formation is the most important and widely exploited.[3,4]

Because of our research interest in synthesizing magnetic complexes, we once found that an in situ C−C coupling reaction occurring at low temperature led to the formation of an antiferromagnetic copper(II) cluster.[5] However, to our best of knowledge, a spin-crossover (SCO) complex, one of the types of magnetic materials, has never been synthesized via an in situ ligand reaction. SCO generally occurs in coordination complexes whose metal ions have a d^4−d^7 electron configuration and usually can be triggered by external stimuli, such as heat, pressure, light, magnetic field, and so on.[6] They may be considered as potential candidates in applications as molecular sensors, molecular switches, information storage, and display devices.[7] Here, we report the temperature-dependent formation of three iron(II) coordination polymers in which the SCO complex **1** is synthesized by the solvothermal method that first involves an in situ ligand C=C coupling.

Experimental Section

Materials and General Method. All solvents and reagents were commercially available and used as received. IR spectra were collected on a Nicolet Avatar 360 FT-IR spectrometer at ambient temperature in KBr pellets in the range of 4000−400 cm^{-1}. Elemental analyses of C, H, and N were performed on a Vario EL III analyzer. The ^1H NMR spectra were recorded at 300 K in a dimethyl-d_6 sulfoxide (DMSO-d_6) solution on a Bruker Advance 400 MHz nuclear magnetic resonance spectrometer, using tetramethylsilane as the internal standard.

Synthesis. N^1,N^2-Bis(pyridin-4-ylmethylene)ethane-1,2-diamine (L). **L** was synthesized by a literature method.[8a] 1,2-Ethylenediamine (10 mmol) and 4-pyridinecarboxaldehyde (20 mmol) were mixed in 50 mL of ethanol (EtOH) and refluxed for 3 h;

*To whom correspondence should be addressed. E-mail: taojun@xmu.edu.cn.

(1) (a) Chen, X.-M.; Tong, M.-L. *Acc. Chem. Res.* **2007**, *40*, 162. (b) Zhao, H.; Qu, Z.-R.; Ye, H.-Y.; Xiong, R.-G. *Chem. Soc. Rev.* **2008**, *37*, 84. (c) Zhang, X.-M. *Coord. Chem. Rev.* **2005**, *249*, 1201.
(2) Blake, J.; Champness, N. R.; Chung, S. S. M.; Li, W.-S.; Schröder, M. *Chem. Commun.* **1997**, 1675.
(3) Hu, S.; Chen, J.-C.; Tong, M.-L.; Wang, B.; Yan, Y.-X.; Batten, S. R. *Angew. Chem., Int. Ed.* **2005**, *44*, 5471.
(4) (a) Li, D.; Wu, T. *Inorg. Chem.* **2005**, *44*, 1175. (b) Li, D.; Wu, T.; Zhou, X.-P.; Zhou, R.; Huang, X.-C. *Angew. Chem., Int. Ed.* **2005**, *44*, 4175.
(5) Tong, J.-P.; Sun, X.-J.; Tao, J.; Huang, R.-B.; Zheng, L.-S. *Inorg. Chem.* **2010**, *49*, 1289.
(6) Gütlich, P., Goodwin, H. A., Eds. Spin Crossover in Transition Metal Compounds I and II. *Topics in Current Chemistry*; Springer: New York, 2004; Vols. *233* and *234*.
(7) (a) Kahn, O.; Kröber, J.; Jay, C. *Adv. Mater.* **1992**, *4*, 718. (b) Kahn, O.; Martinez, C. J. *Science* **1998**, *279*, 44.
(8) (a) Patra, G. K.; Goldberg, I. *Dalton Trans.* **2002**, 1051. (b) Ouyang, X.-M.; Fei, B.-L.; Okamura, T.; Bu, H.-W.; Sun, W.-Y.; Tang, W.-X.; Ueyama, N. *Eur. J. Inorg. Chem.* **2003**, 618.

Published on Web 12/27/2010

Table 1. Crystal Data and Structure Refinement Parameters for Complexes **1a**,**b**−**3**

	1		1a	1b	2	3
formula	$C_{30}H_{28}N_{10}S_2Fe$		$C_{30}H_{28}N_{10}S_2$ Mn	$C_{30}H_{28}N_{10}S_2Zn$	$C_{30}H_{30}FeN_{10}OS_2$	$C_{36}H_{48}Cl_4FeN_{10}O_4S_2$
T (K)	105(2)	250(2)	173(2)	173(2)	173(2)	173(2)
fw	648.6		647.7	658.15	666.61	946.62
space group	$C2/c$		$P2_1/c$	$C2/c$	$Iba2$	$P2_1/c$
a (Å)	19.5642(9)	19.7325(10)	17.3303(13)	24.799(4)	29.549(2)	11.4533(8)
b (Å)	9.5630(5)	9.7062(4)	9.5903(7)	9.6101(3)	12.5168(8)	20.5026(15)
c (Å)	16.072(8)	16.4383(7)	18.8701(17)	16.1899(13)	18.6829(11)	9.3339(6)
β (deg)	96.356(4)	96.432(4)	100.299(8)	126.901(10)		93.353(6)
V (Å^3)	2985.7(3)	3128.6(2)	3085.7(4)	3085.5(6)	6909.9(8)	2188.1(3)
Z	4	4	4	4	8	2
D (g cm^{-3})	1.433	1.377	1.394	1.417	1.303	1.412
μ (mm^{-1})	0.685	0.654	0.602	0.97	0.597	0.734
S	0.948	0.967	0.854	0.973	0.776	1.037
R1/wR2	0.0356/0.0885	0.0382/0.0861	0.0420/0.1160	0.0332/0.0826	0.0464/0.0841	0.0658/0.2038

subsequent evaporation of the solvent gave a yellow powder of **L**, which was washed with *n*-hexane and dried in air. Yield: 80%. IR (KBr, cm^{-1}): 2925, 1687, 1627, 1595, 1550, 1417, 1384, 1310, 1234, 1207, 1121, 1082, 987, 976, 958, 813, 678, 662, 510.

[M(L′)(NCS)$_2$]$_n$ [L′ = 5,6-Dipyridin-4-yl-1,2,3,4-tetrahydropyrazine; M = Fe (1), Mn (1a), Zn (1b)]. A mixture of 0.2 mmol of $FeSO_4$ for **1** ($Mn(ClO_4)_2$ for **1a** and $ZnSO_4$ for **1b**) and 0.4 mmol of KSCN in 2 mL of methanol (MeOH) was stirred for 10 min, then the solution was filtered, and the filtrate was added to 8 mL of a MeOH solution with 0.4 mmol of **L** in a 23 mL Teflon-lined autoclave, which was heated to 130 °C for 72 h to give dark-red block crystals of **1** (orange block crystals of **1a** and red block crystals of **1b**). The crystals were collected by filtration, washed with EtOH, and dried in air. Yield: **1**, ∼20% (**1a**, ∼40%; **1b**, ∼40%). Anal. Calcd for $C_{30}H_{28}FeN_{10}S_2$ (**1**): C, 55.54; H, 4.35; N, 21.61. Found: C, 54.97; H, 4.417; N, 21.51. Anal. Calcd for $C_{30}H_{28}MnN_{10}S_2$ (**1a**): C, 55.63; H, 4.36; N, 21.64. Found: C, 55.11; H, 4.103; N, 21.21. Anal. Calcd for $C_{30}H_{28}ZnN_{10}S_2$ (**1b**): C, 54.87; H, 4.30; N, 21.34. Found: C, 53.46; H, 4.289; N, 21.02. IR (KBr, cm^{-1}) for **1**: 2071, 1609, 1551, 1410, 1399, 1389, 1311, 1214, 1117, 1063, 1034, 1012, 850, 831, 652, 586.

[Fe(L)$_2$(NCS)$_2$]·H$_2$O (2). A total of 0.05 mmol of $Fe(NCS)_2$ was added to 5 mL of a MeOH solution with 0.1 mmol of **L** in a 20 mL glass bottle, which was sealed and heated to 90 °C for 5 days to generate orange block crystals of **2**. The crystals were collected by filtration, washed with EtOH, and dried in air (yield: ∼2%).

[Fe(L)$_2$(NCS)$_2$]·2CH$_2$Cl$_2$·4MeOH (3). A total of 0.2 mmol of **L** was dissolved in 5 mL of CH_2Cl_2, and the solution was put at the bottom of a test tube, upon which 5 mL of a 1:1 (v/v) EtOH−CH_2Cl_2 solution was layered, and then 5 mL of an EtOH solution containing 0.1 mmol of $Fe(NCS)_2$ was carefully layered on the top. Orange block crystals of **3** were obtained after 3 weeks, which were collected by filtration, washed with EtOH, and dried in air (yield: 23%). Anal. Calcd for $C_{34}H_{44}FeN_{10}O_4S_2$: C, 52.56; H, 5.71; N, 18.04. Found: C, 52.06; H, 5.6; N, 18.3. IR (KBr, cm^{-1}): 2924, 2062, 1648, 1610, 1556, 1417, 1384, 1323, 112, 1040, 1006, 832, 808, 640, 619, 536, 520.

Crystallographic Data Collection and Structural Refinement. All diffraction data were collected on an Oxford Gemini S Ultra diffractometer using Mo Kα (λ = 0.710 73 Å) radiation. Data reduction was done with *CrysAlisPro* (Oxford Diffraction Ltd., version 1.171.33.46). Empirical absorption correction used spherical harmonics, implemented in a SCALE3 ABSPACK scaling algorithm. The structures were solved using *SHELXS-97* and refined with *SHELXL-97*.[9] All non-H atoms were refined anisotropically, and H atoms were generated using the riding model. Further details for structural analyses are summarized in Table 1.

Magnetic Measurement. The variable-temperature magnetic susceptibilities were measured at a sweeping rate of 1 K min^{-1} in the range of 2−300 K on a Quantum Design MPMS XL-7 SQUID magnetometer under a magnetic field of 5000 Oe. The pressure effect of the magnetic properties was carried out on an Easy-Lab Mcell 10 hydrostatic pressure cell, which was designed for the MPMS setup with silicone oil as the pressure-transmitting medium. The pressure was applied externally to the sample and measured by the pressure dependence of the superconducting transition temperature of a built-in pressure sensor made of high-purity tin. Magnetic data were calibrated for the sample holder, and diamagnetism was estimated from Pascal's constants.

Results and Discussion

Synthesis. The reaction of N^1,N^2-bis(pyridin-4-ylmethylene)ethane-1,2-diamine (**L**) with $Fe(NCS)_2$ in MeOH at 130 °C for 72 h gave a one-dimensional (1D) complex, [Fe(L′)(NCS)$_2$] (**1**; **L**′ = 5,6-dipyridin-4-yl-1,2,3,4-tetrahydropyrazine), in which the ligand **L**′ formed from the original one (**L**) through an aldimine C=C coupling and cyclization reaction (Scheme 1). It was reported in the literature that a cyanide ion could catalyze such aldimine coupling reactions but gave C−C coupled products.[10] In fact, the cyanide-catalyzed aldimine coupled product is the nitrogen analogue of benzoin condensation, which was first reported by Strain in 1824.[11] In the present case, the mechanism of C=C coupling is proposed as a nucleophilic attack and proton-transfer process, as shown in Scheme 1. The ligand **L**′ was, in fact, an intermediate because a similar reaction occurring in air with a KCN catalyst gave a six-membered ring with C=N and C−C bonds, which indicated that N−H bonds in **L**′ could be further oxidized.[10]

Obviously, the catalyst CN^- ions were generated through decomposition of SCN^- ions. Li et al.[4] reported that inorganic sulfur (SCN^-) could transform into organic sulfur (CH_3S^-) under solvothermal conditions in the presence of MeOH, acetonitrile, and Cu^I ions and subsequently release CN^- ions, in which MeOH and acetonitrile are indispensable. However, **1** was an iron(II) complex that was synthesized with MeOH in the absence of acetonitrile, which indicated that decomposition of SCN^- may be determined by temperature. In order to fully understand

(9) (a) Altomare, A.; Burla, M. C.; Camalli, M.; Cascarano, G. L.; Giacovazzo, C.; Guagliardi, A.; Moliterni, A. G. G.; Polidori, G.; Spagna, R. *J. Appl. Crystallogr.* **1999**, *32*, b115–119. (b) Sheldrick, G. M. *SHELXL-97, Program for refinement of crystal structures*; University of Göttingen: Göttingen, Germany, 1997.

(10) Reich, B.; Justice, E. K.; Beckstead, B. T.; Reibenspies, J. H.; Miller, S. A. *J. Org. Chem.* **2004**, *69*, 1357.

(11) Strain, H. H. *J. Am. Chem. Soc.* **1928**, *50*, 2218.

Scheme 1. Proposed Mechanism of the Dialdimine C=C Coupling

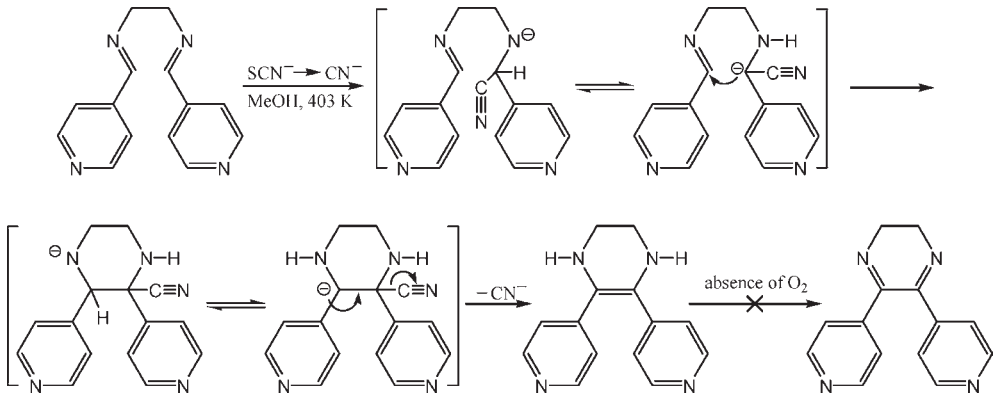

Scheme 2. Syntheses of Complexes **1**−**3**

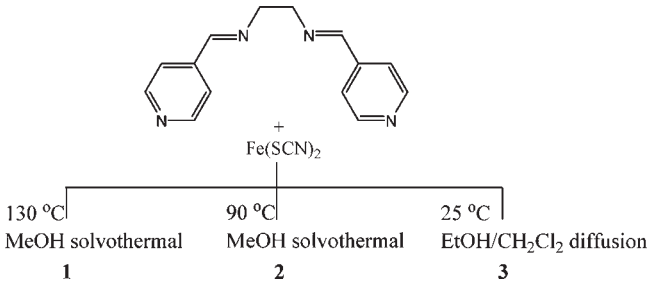

SCN⁻ decomposition, some control experiments were performed, as shown in Scheme 2. At 130 °C for 72 h, **1** with C=C coupling could be obtained in pure MeOH or EtOH or a MeOH−acetonitrile mixture. Instead, replacements of iron(II) salts with manganese(II) and zinc(II) salts could also give the same structures (**1a** and **1b**, respectively) as that of **1**. When the synthesis was conducted at 90 °C, the ligand **L** retained the initial structure and gave a two-dimensional (2D) complex. Furthermore, at room temperature, a similar reaction gave a new 1D complex whose structure is very similar to that of **1** and the ligand **L** also remains intact. Accordingly, we can conclude that the solvothermal conditions are the key point to decomposition of SCN^- ions, and the resultant CN^- ions then catalyze the aldimine C=C coupling. Meanwhile, because of the presence of reductive Fe^{II} ions and ascorbic acid and absence of oxygen in the autoclave, the intermediate product (**L′**) rather than the oxidized one (5,6-dipyridin-4-yl-2,3-dihydropyrazine) was obtained (Scheme 1).

In order to verify the existence of CN^- ions, absorption spectra were investigated. It is presumed that the final CN^- ions in the mixture were coordinated to Fe^{II} ions in the form of $[Fe(CN)_6]^{4-}$, which is easily dissolved in an aqueous solution. The product mixture of **1** was evaporated to dryness and was added to water, the solution was filtered, and the UV−vis spectrum of the filtrate is shown in Figure 1, which clearly indicates the absorbance mode of $[Fe(CN)_6]^{4-}$ in an aqueous solution.[12]

Crystal Structures. Crystallographic data are summarized in Table 1, and selected bond lengths and angles are listed in Tables 2−5. Single-crystal X-ray diffraction data of **1** were collected at 105 and 250 K. Structural analysis

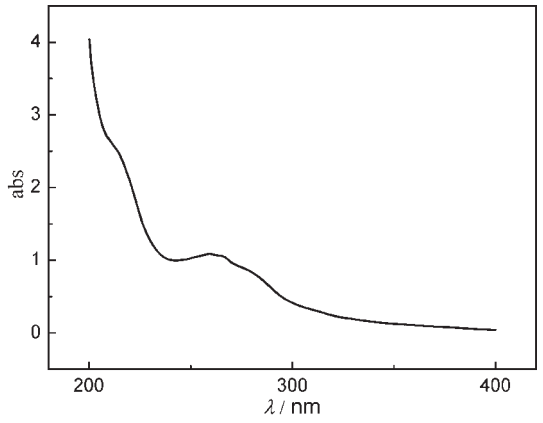

Figure 1. UV−vis data (190−400 nm) of the byproduct mixture of complex **1** dissloved in water.

Table 2. Bond Lengths [Å] and Angles [deg] for **L′** in **1** at 105 K

C5−C6	1.473(3)	C9−C6−N2	120.1(2)
C6−C9	1.365(3)	C9−C6−C5	125.8(2)
C6−N2	1.395(3)	N2−C6−C5	114.1(2)
C7−N2	1.441(3)	C6−C9−N4	120.8(2)
C7−C8	1.521(4)	C6−C9−C10	125.2(2)
C8−N4	1.444(3)	N4−C9−C10	113.9 (2)
C9−N4	1.400(3)		
C9−C10	1.469(3)		

clearly revealed that the ligand **L** was transformed into **L′** via C=C coupling and proton transfer, as shown in Figure 2. At 105 K, the bond length of C6=C9 [1.356(3) Å] is obviously shorter than the C−C single bonds in the ligand [C5−C6 = 1.478(3) Å, C9−C10 = 1.469(3) Å, and C7−C8 = 1.521(4) Å] or the C−C bond [1.517(2) Å] via C−C coupling reactions in ref 10. Meanwhile, C6−N2 [1.395(3) Å] and C9−N4 [1.400(3) Å] (Table 2) are longer than the C=N double bond [1.265(2) Å] in the ligand **L**[8a] or the corresponding C=N bond [1.288(2) Å] in ref 10. The NCC angles involving C6 and C9 are around 120° [120.0(2) and 120.2(2)°, respectively]. So, from the structural point of view, ligand cyclization is achieved through C=C coupling, and therefore the C6−N2 and C9−N4 bonds are single ones attributed to proton transfer from C (C6 and C9) to N (N2 and N4) atoms.

The Fe1 ion is coordinated by six N atoms, four of which in the basal plane of the coordination octahedron are from four **L′** pyridines and the other two of which at the apical position are from two thiocyanate ions. The

(12) Zhang, H. *Coordination Chemistry—Principles and Applications*; Chemical Industry Press: Beijing, 2009; p 214.

Table 3. Selected Bond Lengths [Å] and Angles [deg] for **1** at 250 and 105 K, Respectively[a]

	250 K	105 K
Fe1−N5	2.1088(2)	1.953(2)
Fe1−N5^{a}	2.1088(2)	1.953(2)
Fe1−N1^{a}	2.2122(19)	2.006(2)
Fe1−N1	2.2122(19)	2.006(2)
Fe1−N3^{b}	2.2031(2)	2.014(2)
Fe1−N3^{c}	2.2031(2)	2.014(2)
N5−Fe1−N1^{a}	88.11(8)	92.74(8)
N5^{a}−Fe1−N1^{a}	89.28(7)	88.92(8)
N5−Fe1−N1	89.28(7)	88.92(8)
N5^{a}−Fe1−N1	88.11(8)	92.74(8)
N1^{a}−Fe1−N1	91.68(1)	89.95(10)
N5−Fe1−N3^{b}	88.96(8)	89.73(8)
N5^{a}−Fe1−N3^{b}	93.71(7)	88.63(8)
N1−Fe1−N3^{b}	89.51(7)	89.38(7)
N5−Fe1−N3^{c}	93.71(7)	88.63(8)
N5^{a}−Fe1−N3^{c}	88.96(8)	89.73(8)
N1^{a}−Fe1−N3^{c}	89.51(7)	89.38(7)
N1−Fe1−N3^{c}	176.82(7)	177.42(8)
N3^{b}−Fe1−N3^{c}	89.46(1)	91.41(10)

[a] Symmetry codes: (a) $-x+1, y, -z+{}^{3}/_{2}$; (b) $x, y+1, z$; (c) $-x+1, y+1, -z+{}^{3}/_{2}$.

Table 4. Selected Bond Lengths [Å] and Angles [deg] for **2**[a]

Fe1−N10	2.0941(48)	N8^{b}−Fe1−N9	93.37(17)
Fe1−N9	2.1136(48)	N8^{b}−Fe1−N10	88.42(17)
Fe1−N5	2.1970(48)	N5−Fe1−N9	90.19(18)
Fe1−N8^{b}	2.2117(48)	N5−Fe1−N10	91.59(17)
Fe1−N4^{a}	2.2145(48)	N8^{b}−Fe1−N5	86.56(16)
Fe1−N1	2.2333(48)	N10−Fe1−N1	89.02(17)
		N10−Fe1−N4^{a}	90.25(18)
		N9−Fe1−N1	89.24 (0.17)
		N9−Fe1−N4^{a}	88.06 (0.17)
		N5−Fe1−N4^{a}	92.23 (0.17)
		N1−Fe1−N8^{b}	90.75 (0.16)
		N4^{a}−Fe1−N8^{b}	177.13 (16)
		N4^{a}−Fe1−N1	90.55 (16)

[a] Symmetry codes: (a) $-x, -y+2, z$; (b) $-x+{}^{1}/_{2}, y-{}^{1}/_{2}, z$.

average Fe−N bond length at 250 K is 2.214(2) Å, which corresponds to the high-spin state of the Fe^{II} ion, while at 105 K, it is 2.025(2) Å, shortened by 0.18 Å, clearly indicating the occurrence of a spin transition. When the temperature is decreased from 250 to 105 K, the value of Σ (Σ is defined as the sum of the deviations from 90° of the cis N−Fe−N angles)[13] changes from 18.02(6)° to 13.64(8)°, which is a relatively small change compared to other SCO iron(II) complexes,[16d] and the cell volume reduces by 4.6%. The adjacent Fe^{II} ions are then bridged by the **L**′ ligand through its pyridine groups to form a 1D chain structure, and the chains pack alternately along the *b* axis and are connected to each other through hydrogen bonds formed between the H atoms on tetrahydropyrazine groups of ligand **L**′ in one chain and the S atoms of an adjacent chain to form sheets that possess double layers of chains. The packing style is similar to that reported previously.[14] The manganese and zinc analogues have the same coordination spheres and packing styles as those of complex **1**.

(13) Guionneau, P.; Brigouleix, C.; Barrans, Y.; Goeta, A. E.; Létard, J. F.; Howard, A. K.; Gaultier, J.; Chasseau, D. *C. R. Acad. Sci., Ser. II* **2001**, *4*, 161.

(14) Yang, F.-L.; Li, B.; Hanajima, T.; Einaga, Y.; Huang, R.-B.; Zheng, L.-S.; Tao, J. *Dalton Trans.* **2010**, *39*, 2288.

Table 5. Selected Bond Lengths [Å] and Angles [deg] for **3**[a]

Fe1−N1	2.2494(35)	N5^{a}−Fe1−N4^{c}	90.59 (13)
Fe1−N5	2.1062(36)	N5−Fe1−N4^{c}	89.41 (13)
Fe1−N4^{a}	2.2182(35)	N5^{b}−Fe1−N5	180.00 (6)
		N1^{a}−Fe1−N5^{a}	90.01 (13)
		N1^{a}−Fe1−N5	89.99 (13)
		N4^{b}−Fe1−N4^{c}	180.00 (6)
		N1^{a}−Fe1−N4^{c}	85.96 (13)
		N1^{a}−Fe1−N4^{b}	94.04 (13)
		N1−Fe1−N1^{a}	180.00 (6)

[a] Symmetry codes: (a) $-x-2, -y, -z$; (b) $x-1, y, z$; (c) $-x-1, -y, -z$.

Complex **2** crystallizes in the orthorhombic space group *Iba*2 and also has the FeN_6 coordination core. Similar to **1**, the octahedron of iron is defined by four N atoms from four different ligands **L** and two atoms from two thiocyanate ions (Figure 3). At 173 K, the average Fe−N bond lengths are 2.0941 Å (Fe−NCS) and 2.2141 Å (Fe−L), which correspond to the high-spin state of the Fe^{II} ion. The selected bond lengths and angles are listed in Table 4. The adjacent Fe^{II} ions are bridged by the ligands to form grid units and extend to 2D networks. The 2D sheets are packed layer by layer to generate a supramolecular structure that is the same as its cobalt analogue.[8b]

Complex **3** crystallizes in monoclinic space group $P2_1/c$, which consists of an iron(II) coordination environment similar to that of complex **1** and also possesses similar 1D topology. However, the ligand **L** keeps the original structure, as shown in Figure 4. The packing mode of complex **3** is completely different from that of **1**. The chains simply align parallel to each other to form 2D layers, which are stacked layer by layer to form a 3D supramolecular architecture, in which the cavity is filled by solvent molecules CH_2Cl_2 and MeOH. The average Fe−N bond length of complex **3** is 2.1913 Å, which reveals that the Fe^{II} ions are in the high-spin state.

^{1}H NMR Spectra. The ^{1}H NMR spectra of **L**, **L**′ (in **1b**−Zn), and deuterated **L**′ (in **1b**−Zn) are shown in Figure 5. The peaks at 8.64, 8.38, 7.63, and 3.95 ppm in Figure 5a were assigned to H_α, H_γ, H_β, and H_δ of ligand **L**, respectively. When cyclization occurred, the peaks of H_α, H_β, and H_δ shifted to higher field (Figure 5b). Meanwhile, the peak assigned to H_γ of **L** disappeared and a new peak at 10.21 ppm appeared that is assigned to $H_{\gamma'}$ of ligand **L**′. After deuteration (Figure 5c), the peaks of H_α and H_β remained unchanged and the peak at 3.7 ppm was assigned to the superimposed H_δ of **L**′ and water protons. An obvious change was that the peak of $H_{\gamma'}$ of ligand **L**′ disappeared. This confirms the coupling mechanism and suggests that the N−H protons are active and can be substituted by deuterium.

Magnetic Properties. The $\chi_M T$ versus T plots of complex **1** are shown in Figure 6a (black squares for atmospheric pressure). The $\chi_M T$ value at room temperature is 3.76 cm^3 K mol^{-1}, higher than that expected for a spin-only high-spin Fe^{II} ion. The $\chi_M T$ value remains constant upon cooling to 175 K and then decreases abruptly to reach a value of 1.29 cm^3 K mol^{-1} at 56 K. Between this temperature and 16 K (1.26 cm^3 K mol^{-1}), there exists a distinct plateau. This behavior evidently indicates the occurrence of a continuous and thermally dependent incomplete spin transition. As the temperature further decreases, the $\chi_M T$ value suddenly decreases to a value of 0.77 cm^3 K mol^{-1}

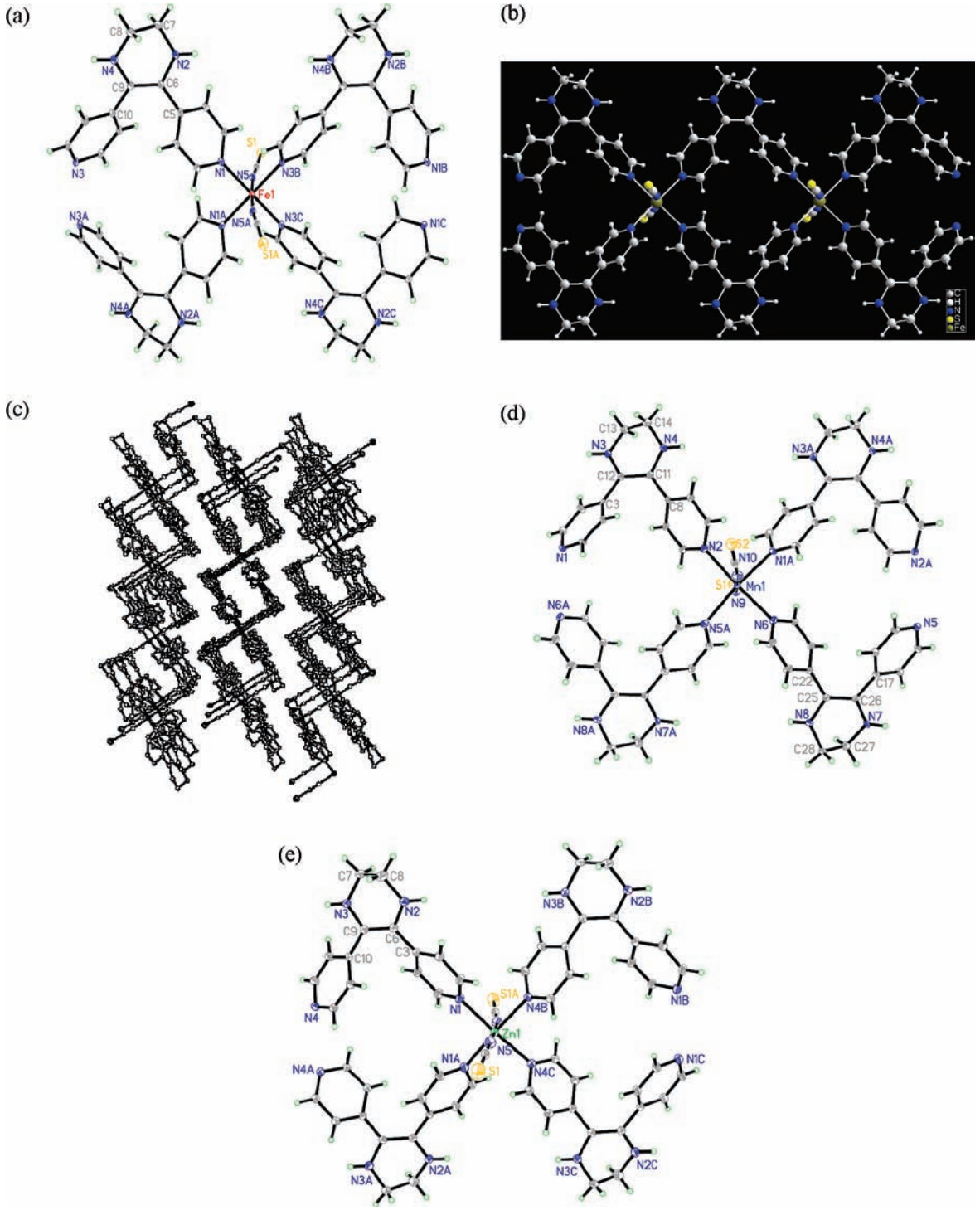

Figure 2. (a) Perspective view of the coordination environment of the Fe^{II} ion in **1** drawn at 35% thermal ellipsoid probability. Symmetry codes: (A) $-x+1, y, -z+{}^{3}/_{2}$; (B) $x, y+1, z$; (C) $-x+1, y+1, -z+{}^{3}/_{2}$. (b) Chain structure of **1**. (c) View of the 3D structure of **1** along the *b* axis. (d) Perspective view of the coordination environment of the Mn^{II} ion in **1a**−Mn drawn at 30% thermal ellipsoid probability. Symmetry codes: (A) $x, y+1, z$. (e) Perspective view of the coordination environment of the Zn^{II} ion in **1b**−Zn drawn at 30% thermal ellipsoid probability. Symmetry codes: (A) $-x-1, y, z+{}^{1}/_{2}$; (B) $x, y+1, z$; (C) $-x-1, y+1, -z-{}^{1}/_{2}$.

at 2 K, which is most likely caused by the effects of zero-field splitting of the residual high-spin (∼34% calculated from the values at 300 and 56 K) Fe^{II} populations. At temperatures below 16 K, the antiferromagnetic interactions between the residual high-spin Fe^{II} populations through the **L′** ligands may also play an important role in causing the sudden decrease. The incomplete feature of a spin transition is also observed in the chainlike coordination polymer with a similar bipyridyl V-shaped linker[14] and a family of 1D coordination polymers with the 2-(2-pyridyl)-imidazole ligand and bipyridyl linear bridging ligands.[15] On the other hand, several 2D gridlike coordination polymers built with bipyridyl ligands also showed incomplete spin transitions.[16]

Because the rigid 1D structure and the spin-transition behavior resemble those of a 2,4,5-tris(4-pyridyl)imidazole

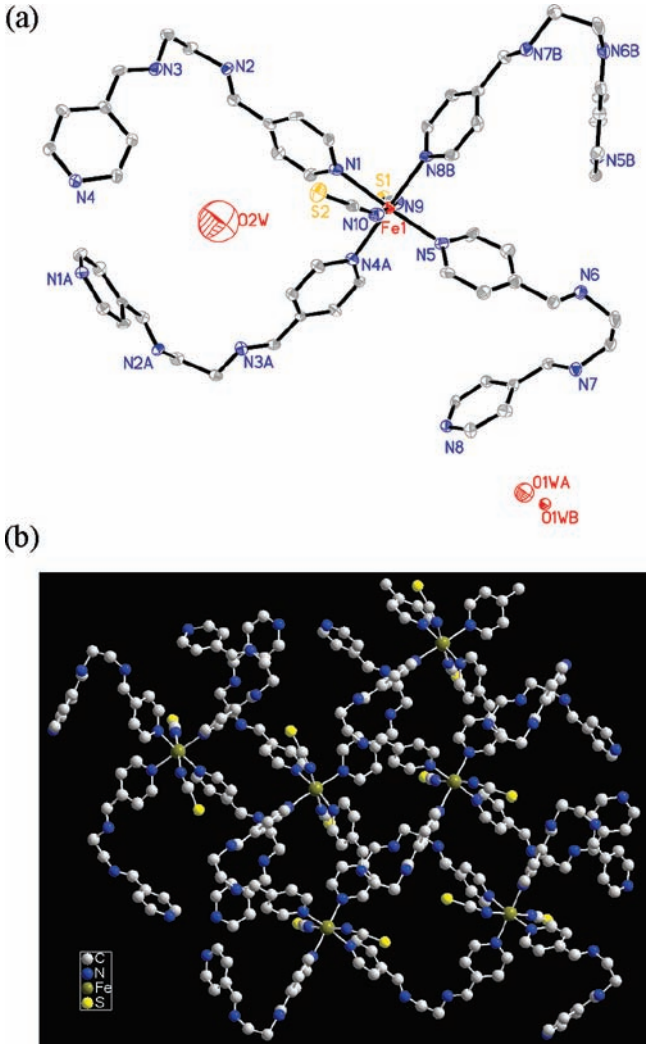

Figure 3. (a) Perspective view of the coordination environment of the Fe^{II} ion in **2** drawn at 30% thermal ellipsoid probability. The H atoms have been omitted for clarity. Symmetry codes: (A) $-x+2, y, z$; (B) $-x+{}^1/_2, y-{}^1/_2, z$. (b) View of the 2D structure of **2**. H atoms, thiocyanate ions, and solvent molecules have been omitted for clarity.

iron(II) complex,[14] we anticipate that the spin transition of complex **1** would also be sensitive to pressure, such as for a large number of SCO complexes studied in this regard.[17] As shown Figure 6a, we can find that at room

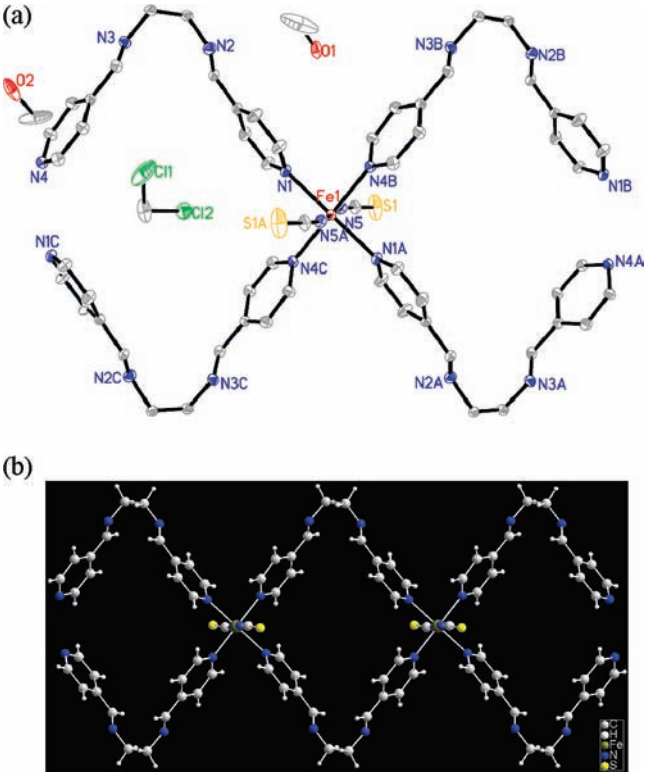

Figure 4. (a) Perspective view of the coordination environment of the Fe^{II} ion in **3** drawn at 30% thermal ellipsoid probability. The H atoms were omitted for clarity. Symmetry codes: (A) $-x+2, -y, -z$; (B) $x-1, y, z$; (C) $x+{}^1/_2, -y, -z$. (b) Chain structure of **3**.

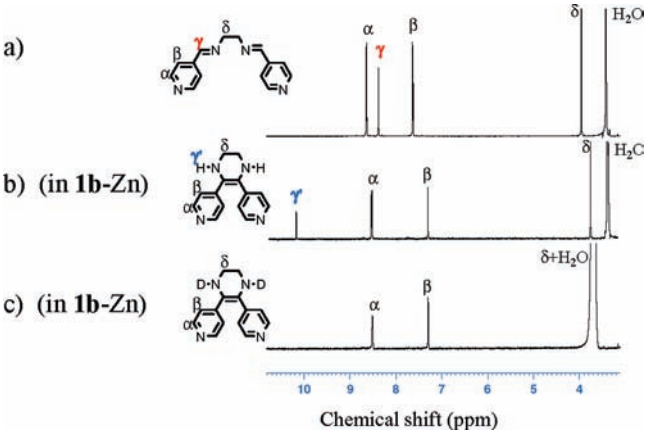

Figure 5. ^{1}H NMR spectra (400 MHz, DMSO-d_6, 300 K) of ligand **L** (a), ligand **L′** (in **1b**−Zn), (b) and deuterated **L′** (in **1b**−Zn) (c).

temperature the high-spin populations under 0−6.62 GPa remain almost unchanged, which is unexpected because it is well-documented that external pressure favors low-spin states and reduces high-spin populations in most SCO complexes.[18] Only at extremely high pressure (9.89 GPa) does the room temperature high-spin population reduce by ~18%. On the other hand, at the low-temperature range, the plateau (1.26−1.29 cm^3 K mol^{-1}) between

(15) (a) Matouzenko, G. S.; Molnár, G.; Bréfuel, N.; Perrin, M.; Bousseksou, A.; Borshch, S. A. *Chem. Mater.* **2003**, *15*, 550. (b) Matouzenko, G. S.; Perrin, M.; Le Guennic, B.; Genre, C.; Molnár, G.; Bousseksou, A.; Borshch, S. A. *Dalton Trans.* **2007**, 934.

(16) (a) Real, J. A.; Andrés, E.; Muñoz, M. C.; Julve, M.; Granier, T.; Bousseksou, A.; Varret, F. *Science* **1995**, *268*, 265. (b) Moliner, N.; Muñoz, M. C.; Létard, S.; Solans, X.; Menéndez, N.; Goujon, A.; Varret, F.; Real, J. A. *Inorg. Chem.* **2000**, *39*, 5390. (c) Real, J. A.; Gaspar, A. B.; Niel, V.; Muñoz, M. C. *Coord. Chem. Rev.* **2003**, *236*, 121. (d) Neville, S. M.; Halder, G. J.; Chapman, K. W.; Duriska, M. B.; Southon, P. D.; Cashion, J. D.; Létard, J. F.; Moubaraki, B.; Murray, K. S.; Kepert, C. J. *J. Am. Chem. Soc.* **2008**, *130*, 2869.

(17) (a) Ksenofontov, V.; Levchenko, G.; Spiering, H.; Gütlich, P.; Létard, J.-F.; Bouhedja, Y.; Kahn, O. *Chem. Phys. Lett.* **1998**, *294*, 545. (b) Gütlich, P.; Gaspar, A. B.; Ksenofontov, V.; Garcia, Y. *J. Phys.: Condens. Matter* **2004**, *16*, S1087. (c) Agustí, G.; Gaspar, A. B.; Muñoz, M. C.; Real, J. A. *Inorg. Chem.* **2007**, *46*, 9646. (d) Bai, Y.-L.; Tao, J.; Huang, R.-B.; Zheng, L.-S.; Zheng, S.-L.; Oshida, K.; Einaga, Y. *Chem. Commun.* **2008**, 1753. (e) Létard, J.-F.; Carbonera, C.; Real, J. A.; Kawata, S.; Kaizaki, S. *Chem.—Eur. J.* **2009**, *15*, 4146. (f) Li, B.; Wei, R.-J.; Tao, J.; Huang, R.-B.; Zheng, L.-S. *Inorg. Chem.* **2010**, *49*, 745.

(18) (a) Hattacharjee, B.; Koningsbruggen, P. J.; Hibbs, W.; Miller, J. S.; Gütlich, P. *J. Phys.: Condens. Matter* **2007**, *19*, 406202. (b) Genre, C.; Jeanneau, E.; Bousseksou, A.; Luneau, D.; Borshch, S. A.; Matouzenko, G. S. *Chem.—Eur. J.* **2008**, *14*, 697.

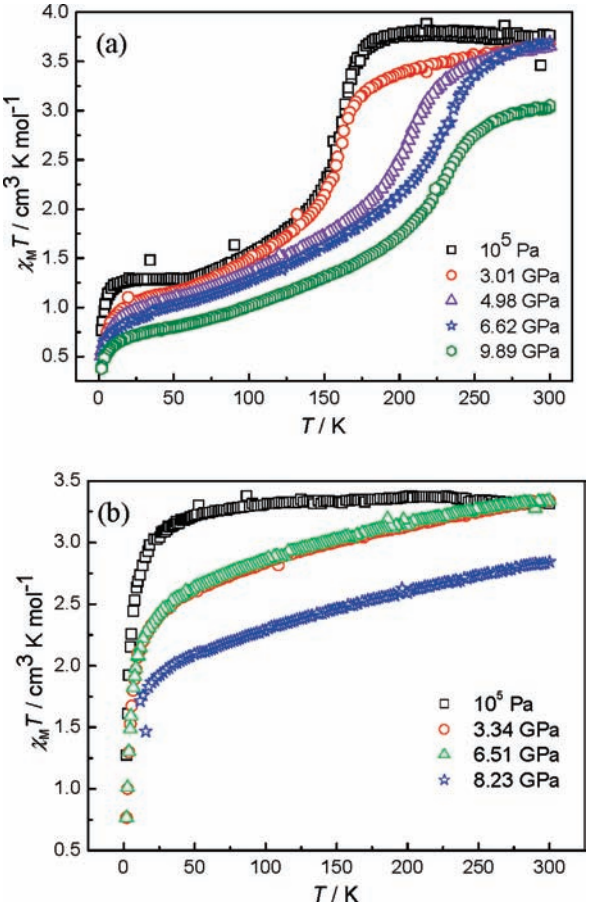

Figure 6. $\chi_M T$ versus T plots of **1** (a) and **3** (b) under variable pressure (H = 0.5 T).

16 and 56 K under atmospheric pressure generally disappears accompanied with increasing pressure. Meanwhile, the spin transition remains incomplete under available pressure as large as 9.89 GPa, and the percentage of the high-spin state deduced from the susceptibility values at 50 K is about 20%. Under external pressure, the primary changes mainly take place in the temperature range of 60−250 K, where the relatively steep transition under atmospheric pressure and 3.01 GPa becomes more and more smooth and the critical temperature shifts to a higher temperature range upon increasing pressure.

Complex **2** is paramagnetic, as evidenced by the bond lengths of Fe−N at 173 K. Similar 2D gridlike iron(II) complexes with bridging ligands 1,2-di-4-pyridylethane[19b,e] and 1,3-di-4-pyridlypropane[19f] were also paramagnetic and may display SCO behavior by enclathrating suitable organic molecules[19c] or replacing NCS^- with $NCBH_3^-$. Complex **3** is also paramagnetic, as shown in Figure 6b. Different from that of **1**, the non-SCO properties of **2** and **3** may be due to the loose packing structures or encapsulation of unsuitable solvent molecules. Margarita et al.[19a] reported that a 1D architecture similar to that of ligand 1,2-di-4-pyridylethane is paramagnetic and could undergo SCO by enclathrating selected organic guest molecules.[19b] The pressure-dependent properties of **3** were used; the results suggested that **3** remained at a high-spin state even at 8.6 GPa (Figure 6b), and the reason may be that **3** is composed of a more flexible ligand than **1** that counteracts the effect of the pressure.

Conclusion

We reported the synthesis of three iron(II) coordination polymers in which complex **1** was formed by an in situ ligand C=C coupling reaction that is confirmed to be temperature-dependent and driven by the catalyst CN^- decomposed from SCN^-. Magnetic studies indicate that **1** shows a temperature- and pressure-dependent incomplete spin transition, whereas **2** and **3** with the similar coordination environment around the Fe ions exhibit high-spin states in the whole temperature range.

Acknowledgment. This work was supported by the NNSF of China (Grants 90922012, 20971106, and 20721001), NCET-08-0470 of MOE, the NSF of Fujian Province for Distinguished Young Scientists (Grant 2009J06006), and the National Basic Research Program of China (973 program, Grant 2007CB815301).

Supporting Information Available: Crystallographic data in CIF format. This material is available free of charge via the Internet at http://pubs.acs.org.